Available online www.unicrossjournals.com

UNICROSS JOURNAL OF SCIENCE AND TECHNOLOGY, UJOST

RESEARCH ARTICLE VOL. 4(3) SEPTEMBER, 2025 ISSN:2814-2233

Date Approved September 30, 2025 Pages 90 – 122

LITHO–SURFICIAL AND SOURCE PROXIMATE ANALYSIS OF AIRBORNE URANIUM CONCENTRATION IN WESTERN PART OF OGUN STATE, NIGERIA

Ogunsanwo, F.O
Physics Department,
Tai Solarin University of Education,
Ijagun, Ogun State Nigeria
Phone Number: Email: ogunsanwofo@tasued.edu.ng

Abstract

Uranium has been found to be one of the radioactive element emanating from the earth subsurface and is mobile in nature. Its distribution is controlled by the stratigraphic layer and overburden thickness of earth crust. In this study, the airborne uranium concentration distribution in western part of Ogun state was examine across twelve lithological units (LT1 – LT12). The 2D contour plot and 3D surface plot were constructed for each lithological unit to visualize the nature and pattern of the uranium distribution. The source proximate of lithological units were assessed by subjecting the uranium concentration in each unit to inferential statistical and multivariate statistical analysis. Two inferential analysis were employed; namely, F–test and T–test while Principal component analysis (PCA) and Hierarchical cluster analysis (HCA) were adopted for multivariate statistics. Histogram distribution was as well constructed for uranium concentrations across the twelve lithological units. The spatial mapping revealed uranium concentration to be in abundance in study areas with maximum value of 15.0 ppm in LT1 and LT6. Numerous spots of anomalous uranium response to underlying bedrock were identified with the surficial construction with different migration patterns. F–test and T–test result revealed LT6 to have different uranium source from the six other lithological units. Five PCA were identified, with all units positively loaded, except LT6. Three clusters were obtained with LT6 having distinct cluster with others. The histogram distribution revealed multimodal pattern in most uranium lithological unit, while LT6 have minimal source. This study have critically assessed the uranium concentration in Western part of Ogun state structurally and progenically, with reliable evidence of its abundance deposition which is mostly controlled by the underlying bedrocks.

Key words: Uranium; Inferential; Cluster; Lithological; Sources

1.0 Introduction

Airborne geophysical surveys (including airborne gamma-ray spectrometry) are critical for regional geological mapping and mineral resource assessment, particularly in data-scarce regions like parts of Nigeria (Telford, et al., 1990; Oladunjoye, et al., 2016; Abdulsalam, et al., 2023; Ogungbemi, et al., 2021). These surveys enable efficient detection of uranium, thorium, and potassium distribution across expansive terrains and aid in identifying potential mineralized zones (Paul et al 2022, Wara, et al., 2021; Faruwa et al., 2021).

Specifically, in southwestern Nigeria, Ogun State included, aviation surveys have been conducted under the "Pilot Project" and Phase I airborne geophysical programs by the Nigerian Geological Survey Agency (NGSA), generating comprehensive magnetic and radiometric datasets that form the foundation for exploring uranium and other critical resources (NGSA, 2019; Ogunsanwo, et al., 2019).

Ogun State lies within parts of Nigeria's basement complex, yet early aeroradiometric investigations have revealed significant uranium anomalies not only in granitic terrains but also within sedimentary and weathered zones , particularly across shale, sandstone, and migmatite-bearing formations (Okeyode and Olurin, 2018; Adewoyin, et al., 2019, Jegede et al., 2025). Within the broader north-central uranium-bearing belt, radiometric anomalies have been documented in multiple exposures (Adegoke and Omatsola, 2015; Ezekiel and Nur, 2023), including sheets in Ogun and adjacent regions, pointing to stratigraphic and structural controls on uranium mineralization (Oladunjoye and Ademila, 2015).

Recent studies underscore the value of advanced statistical tools in interpreting uranium geophysical datasets (Ologe, et al., 2024; Ezekiel and Nur 2023; Idi et al 2021; Ngwaka, et al., 2023; Onyejiuwaka, and Nkiru, 2020; Ogunsanwo, et al., 2021) highlighting the importance of lithological context and spatial continuity in understanding uranium distribution.

The major objectives of this study are to:

(i) Characterize the **surficial distribution** of airborne uranium concentrations linked to lithological units.
(ii) Apply **source-proximate analysis** to relate geophysical signals to geological units and structures (basement exposures, weathered zones, sedimentary cover).
(iii) Integrate **lithological mapping** with spatial uranium anomalies to distinguish between primary lithological controls and secondary, structurally or weathering-induced remobilization.

The current study adopts geospatial construction and source proximity-based approaches to parse litho-surficial controls on uranium concentration. By delineating the lithological sources of uranium and mapping their spatial relationships, this work seeks to refine exploration targeting and improve understanding of uranium mobility within the complex surficial and regolith environment of the region.

2.0 Materials and methods

2.1 Geological description of the study area

The study area is situated between latitudes 6°58′11″N and 7°59′27″N, and longitudes 2°44′47″E and 3°20′15″E of the Greenwich meridian, covering a total landmass of approximately 11,183.6 km². It is bounded by Oyo State to the north and the Republic of Benin to the west (Figure 1). Geologically, the region is dominated by two major rock assemblages: the Precambrian Basement Complex in the northern sector, comprising both older and younger granites, and the sedimentary successions of Cretaceous to Tertiary age in the southern sector (Omatsola & Adegoke, 1981; Badmus, et al., 2010). Within the Dahomey Basin, three prominent lithostratigraphic formations are identified due to their genetic and lithological affinities: the Abeokuta Formation (central part), the Ewekoro Formation (south of the Abeokuta Formation), and the Ilaro Formation (southernmost part). Structurally, the area is characterized by fault and fracture patterns associated with the Crystalline Basement Fracture System, notably the Ibadan–Abeokuta fracture zone (Rahaman, 1976; Kogbe, 1989; NGSA, 2019).

2.2 Airborne data Collection

A gridded uranium concentration map covering the northwestern part of Ogun State, Nigeria, was obtained from the aeroradiometric archives of the Nigerian Geological Survey Agency (NGSA), Abuja. The uranium dataset was acquired using an airborne 256-channel gamma-ray spectrometer with an energy window range of 1.66–1.86 MeV (NGSA, 2022). Uranium (^{238}U) concentrations were indirectly determined through measurements of its daughter radionuclide, ^{214}Bi, within the decay series. Under the conventional assumption of secular equilibrium within the uranium decay chain, these measurements are expressed as equivalent uranium (eU) in parts per million (ppm).

By integrating the geological map of the area with the uranium grid data, twelve lithologically defined uranium units (ULT1–ULT12) were delineated (Figure 1; Table 1). From the gridded dataset, a total of 264,844 uranium data points were extracted and spatially partitioned into the defined LT units according to their geological coordinates. This subdivision enabled the identification of lithological units exhibiting proximate anomalous uranium responses, thereby providing a framework for evaluating the litho–surficial controls on uranium distribution.

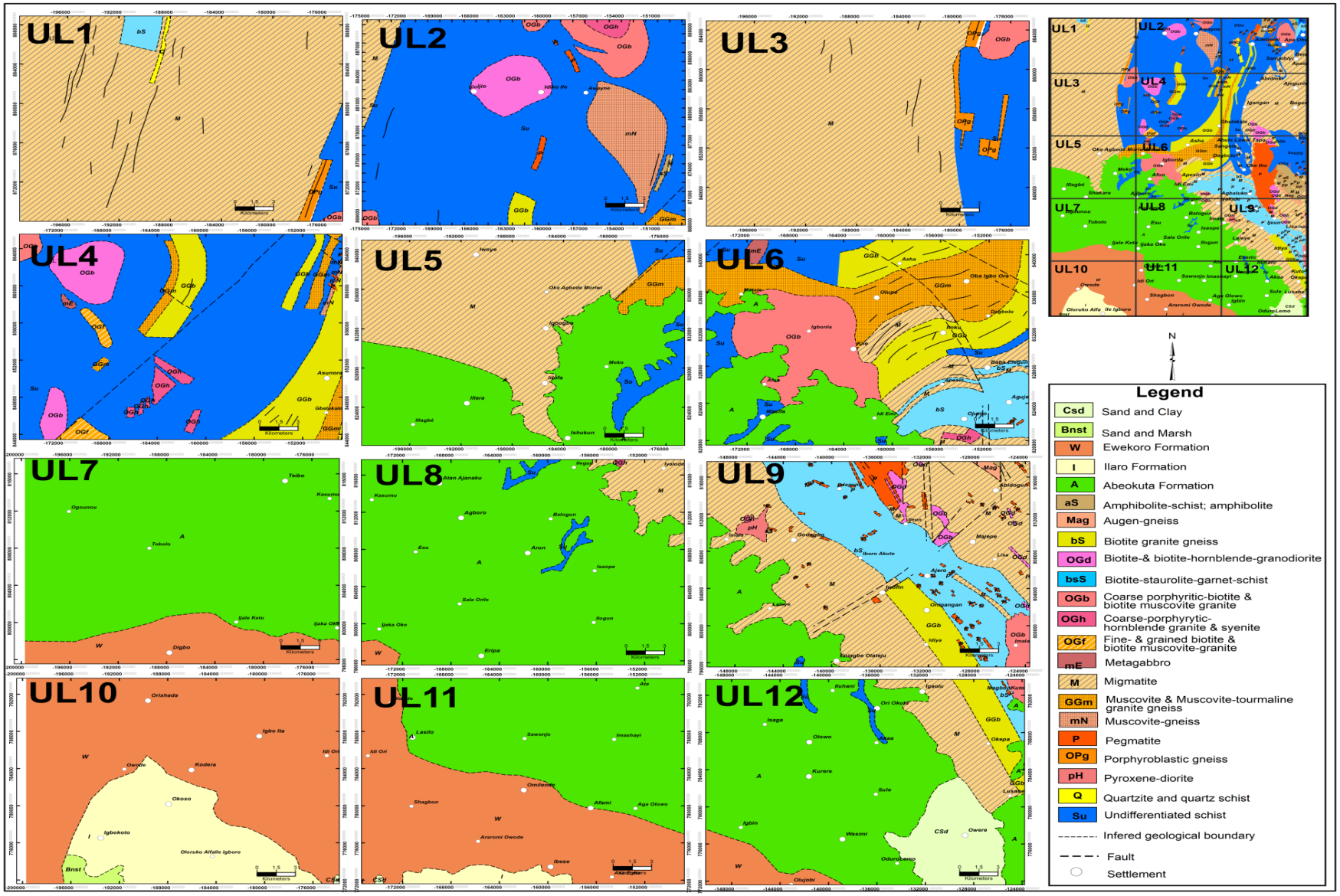

Figure 1: Partitions extracted from geological map showing the bedrock composition of the 12 uranium lithological units (ULT1 – ULT12)**.**

Table 1: Lithological classifications, uranium data and Stratified rock units.

Lithological Units	Nsample	Formation	Stratified rock units
ULT1	11465	Basement	M + OPg+OGb+Q+ bS +Su
ULT2	240	Basement	M+ Su+GGb+aS+GGm +P+OGb +OGh+mN
ULT3	20690	Basement	M + Su + OGb+ OPg
ULT4	13276	Basement	OGb+Su+ P + GGb +GGm+OGh+mN+OGf+mE
ULT5	14666	Weathered Basement	M+ Su ++ Sh + GGm+ Sdt
ULT6	26029	Weathered Basement	M+ Su + bS+OGh+OGb+GGm+ Sh+mE+OGf
ULT7	15903	Sedimentary	Sdt + Lm + Sh
ULT8	39933	Weathered Basement	M+Su+OGh +Sdt + Lm + Sh
ULT9	26543	Weathered Basement	M+P+OGb+Mag+OGd+aS+Std+bS+Sh+OGh+ pH+GGb
ULT10	16099	Sedimentary	Bnst + Sdt + Csd+ Sh + Lm
ULT11	40000	Sedimentary	Sdt + Csd + Sh + Lm
ULT12	40000	Weathered Basement	M + Csd + Sdt +Lm + A+ Sh +bS + GGb + P

M-Migmatite, bS-Biotite staurollite garnet schist, Su-Undifferentiated Schist, OGb-Coarse porphyritc biotite and biotite muscovite granite, mN-Muscovite gneiss, OGh--Coarse porphyritc hornblende granite and syenite, bS- Biotite granite gneiss, OPg- Porphyroblastic gneiss, GGm-Muscovite and muscovite tourmaline granite gneiss, Csd- Clay and sand, Sh-Shale, mE-Metagabrro, OGf- fine grained biotite and biotite muscovite granite, Sdt-Sandstone, P- Pegmatite, Mag-Augen gneiss, Bnst- Sand and Marsh, Lm-Limestone, A- Alluvium.

2.3 Data Analysis

2.4 2D and 3D mapping of uranium concentration

The 2D and 3D uranium map were constructed by subjecting the gridded uranium concentration in XYZ to MatLAB program code. The minimum and maximum value of X and Y were estimate for each lithological unit and fit to flight spacing between 250 – 500m. The uranium data set (Z components) was mesh grid using scattered interpolant to generate the 2D and 3D map.

2.5 Inferential Statistics

In this study, two inferential statistical analysis, namely F – test and T – test were adopted to examine the relationship between the uranium anomalous sources across the twelve lithological units. In order to achieve this, two sets of hypotheses as proposed by Ammar et al (1988); Youssef (2016); Ogunsanwo et al (2023) to ascertain the interdependency of uranium sources from lithology to lithology.

H_0: There **is a significant relationship** between uranium concentration and lithological units obtained from the airborne surveys (Single or common sources).

H_1: There **is a no significant relationship** between uranium concentration and lithological units obtained from the airborne surveys (Multiple sources).

If computed value < critical value, then H_0 hypothesis will be accepted. Conversely, if the computed value > critical, the H_0 hypothesis is rejected, while H_1 is adopted

2.5.1 The Fisher's (F-*) Test.*

The Fisher's test permits testing the null hypothesis that the variances of the parent populations of two samples are identical (or at least equal). In this study, the F-test was carried out in accordance with Ogunsanwo et al (2019)

2.5.2 Student's *t*-Test

The Student's *t*-distribution is a statistical tool commonly employed to test hypotheses concerning the difference between the arithmetic means of two independent samples drawn from normally distributed populations with equal variances. Under the assumption of normality and homogeneity of variance, the test statistic follows a *t*-distribution with $(n_1 + n_2 - 2)$ degrees of freedom, where n_1 and n_2 represent the sample sizes.

When the equality of variances is assumed, the sample variances (S_1^2 and S_2^2) are pooled to provide a single, more robust estimate of the population variance (Sp^2). This pooled variance serves as the basis for computing the *t*-statistic, which is then evaluated against critical values of the *t*-distribution to determine the significance of the observed difference between sample means.

In this study, the *t*-test was applied to evaluate the statistical significance of mean differences, following the procedure outlined by Ogunsanwo et al. (2019).

2.6 Multivariate Statistical Analysis

In this study, the uranium concentrations across the lithological units were subjected to two multivariate statistical analysis; namely; Principal component analysis (PCA) and Hierarchical cluster analysis (HCA). This was conducted to estimate the proximal sources of the uranium concentration and established their relationship with one another.

2.7 Histogram distribution of uranium concentrations

In this study, the histogram was constructed to study the distribution pattern of the uranium concentrations obtained from the airborne survey across the twelve lithological units in the western part of Ogun State. The essence of this is to investigate the normal and asymmetric nature of

the used uranium anomalous responses across the lithological units.

3.0 Results and Discussion

3.1 Spatial mapping of Lithological units

The spatial distribution of the uranium concentration were visualized in 2D contour and 3D surface plot for LT1 – LT12 across the study area (Figures 2 – 13). The petrological classification of the lithological unit (Table1) revealed four basement unit (LT1, LT2, LT3 and LT4), five weathered basement unit (LT5, LT6, LT8, LT9 and LT12) and three sedimentary unit (LT7, LT10 and LT11).

In LT1, the spatial representation of uranium concentration (Fig 2a) depicts low prevalence in the upper NW part. The high concentration was found in the central part and upper NE section of the unit with maximum value of 15ppm. The structural response of uranium to the geological composition (Fig. 2b) revealed low steep response in the NW corner and elevated high peaked uranium at the NE and western part of the unit. LT2 unit (Fig. 3a) accounted for low uranium distribution in the upper and lower part of the unit and relative high concentration around NE part of the unit with maximum value of 7.5ppm. Structurally, the surface response revealed that uranium in LT2 (Fig 3b) tend to have linear sharp steep for lower concentrations.

The spatial representation in LT3 (Fig. 4a) revealed maximum concentration of 6 ppm with relative low concentration in the SW corner, SS, N – S and SE corner. Structurally, the moderate and high concentration region are relatively peaked while the low concentration appears to be steep in the NE and SS part of the unit. The host rock may be extrusive in nature appearing like outcrop across the lithological unit. LT4 spatial distribution of uranium (Fig. 5a) show moderate concentration around western trending to the central part and at the upper northern part of the unit. The low concentration predominantly engulf the unit alongside high concentration around NE corner. The maximum uranium concentration in the unit is 14 ppm. Tectonically, the moderate concentration appears to be slightly elevated while the low concentration tend to be uniformly distributed across the entire unit with slight topographical elevation (Fig. 5b). A sharp peaked elevated high uranium concentration is associated with sharp anomalous response around NE corner.

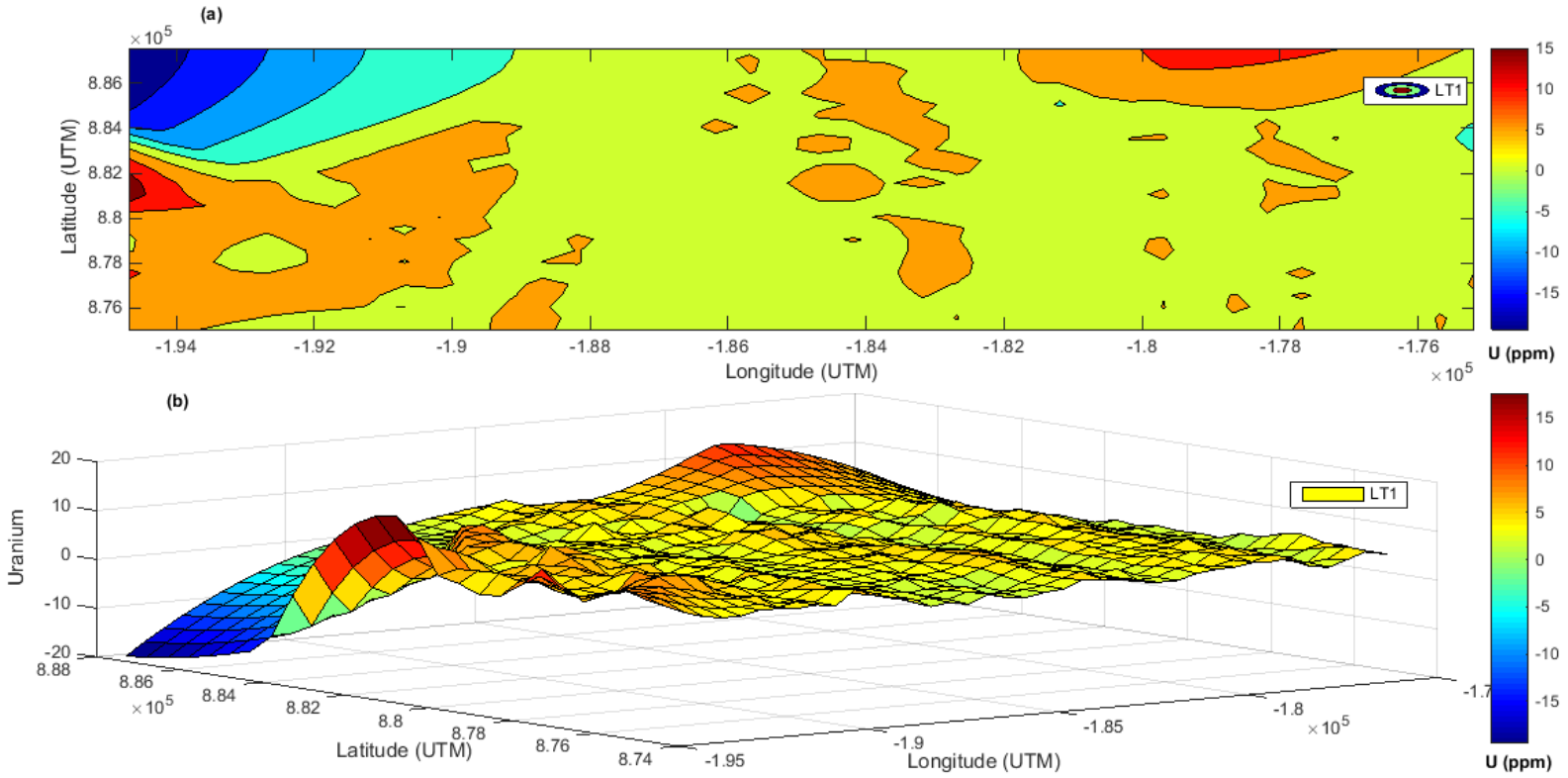

Figure 2: Spatial Surficial representation of uranium distribution in (a) 2D contour (b) 3D surface form of LT1 unit

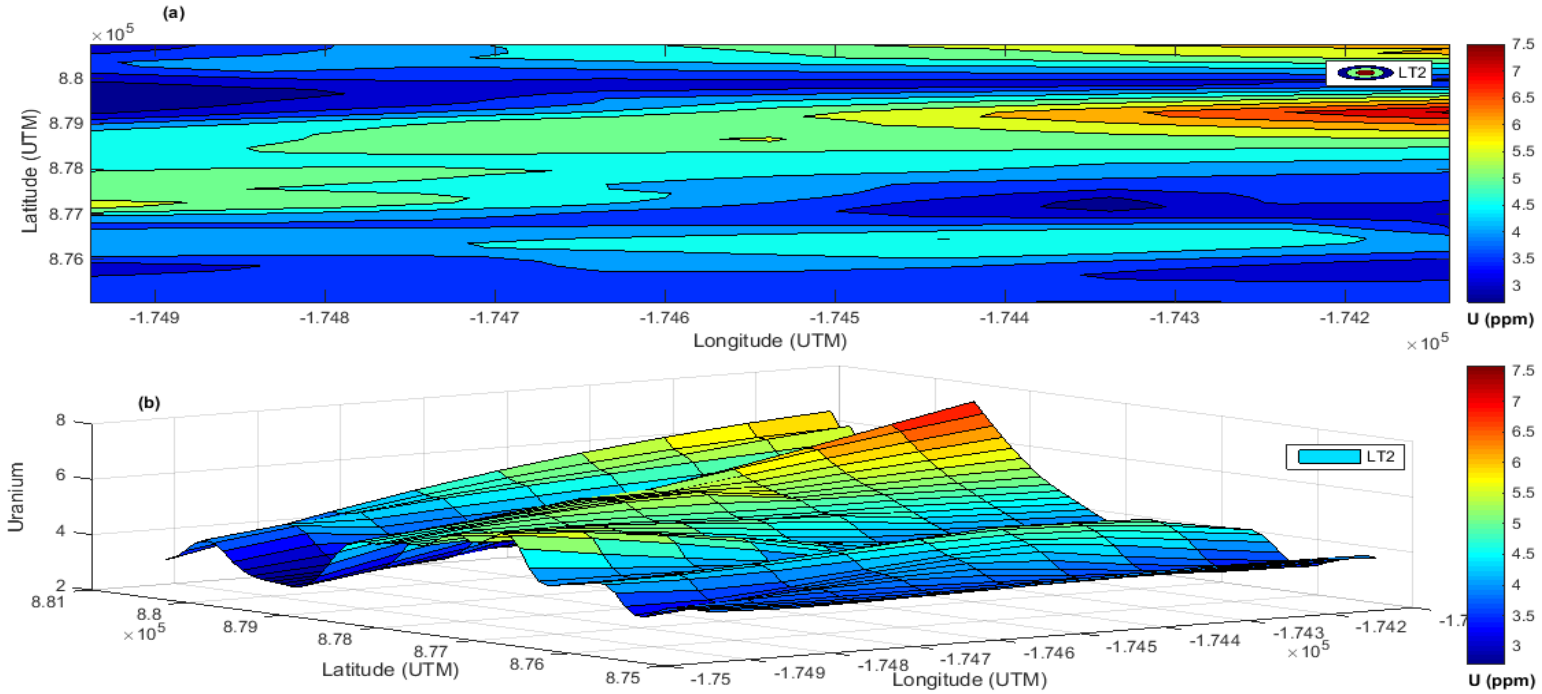

Figure 3: Spatial Surficial representation of uranium distribution in (a) 2D contour (b) 3D surface form of LT2 unit

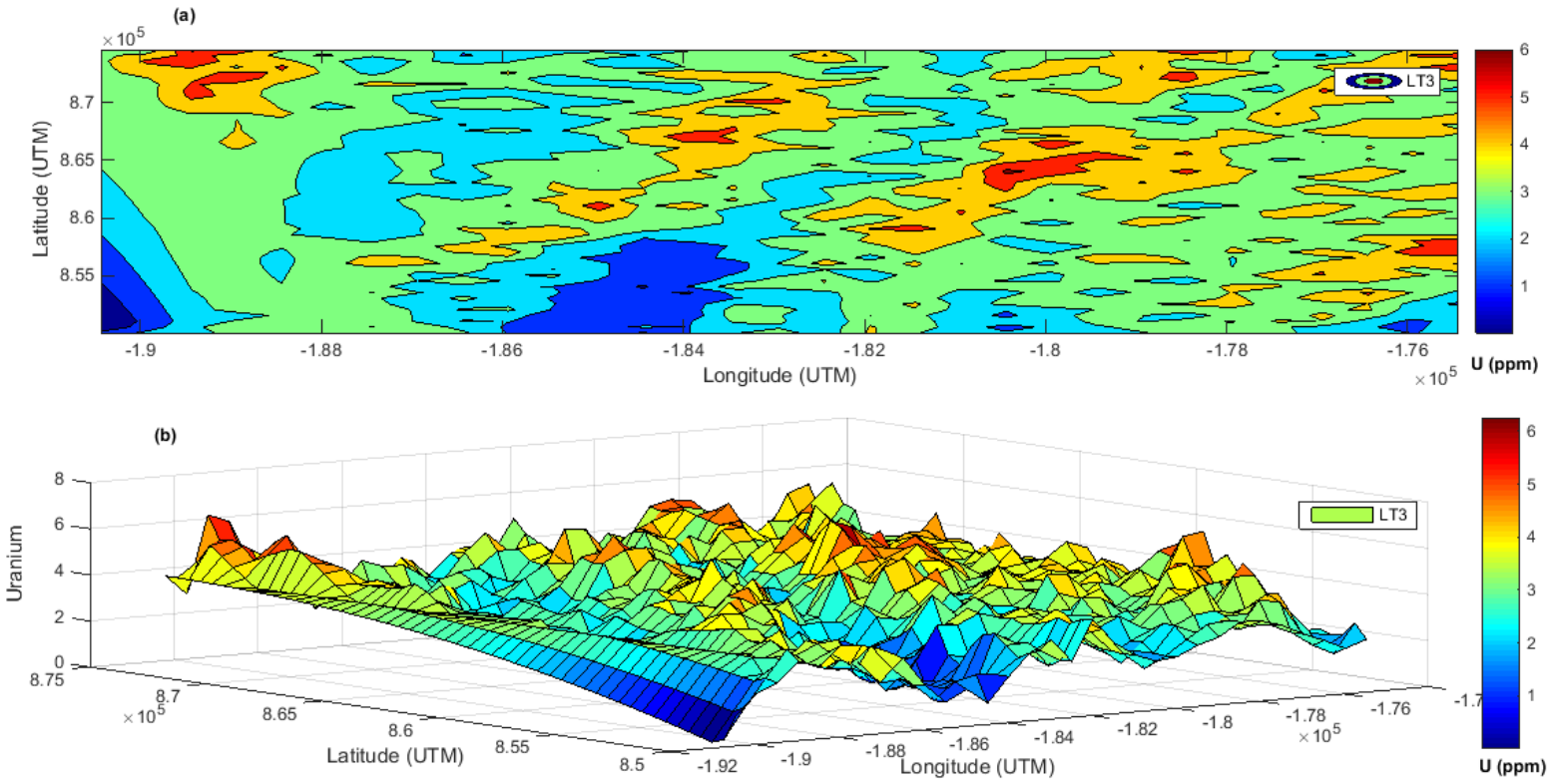

Figure 4: Spatial Surficial representation of uranium distribution in (a) 2D contour (b) 3D surface form of LT3 unit

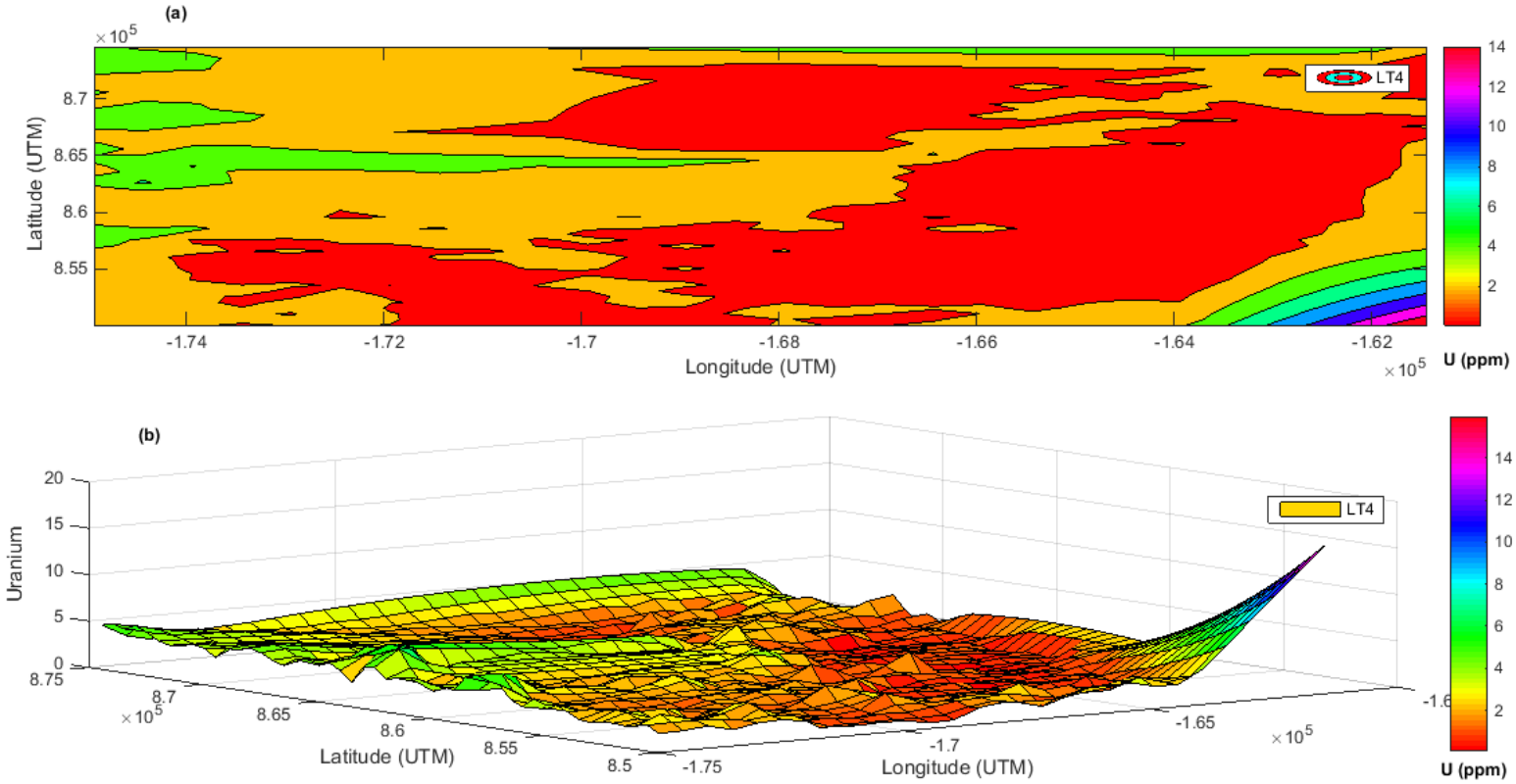

Figure 5: Spatial Surficial representation of uranium distribution in (a) 2D contour (b) 3D surface form of LT4 unit

In the LT5 unit (Fig. 6a), the low to moderate uranium prevalence was observed trending centrally – SS – NE – Eastern part of the unit. The W – SW part of the unit depict relative high uranium concentration with maximum value of 10 ppm. Structurally, the elevated uranium concentration in the W – SW part appears to be segmented and topographically elevated (Fig. 6b). The moderate – high uranium in the eastern part are highly peaked compared to the region of low concentration in the unit. The spatial distribution in The LT6 unit (Fig. 7a) depict high uranium concentration dominance in the upper NE section with maximum value of 15 ppm. The uranium lower concentration was found in the eastern part of the unit while the moderate dominance was found in most part of the unit. Relative high uranium concentration was found in the Central Trending W – SS part of the unit. Structurally (Fig. 7b), the upper NE experienced high shoot out in the uranium concentration while the moderate to relatively high concentration in the most part of the lithological unit tend to be uniform but with few relative sharp peak points. The low concentration section depicts downward narrow steep feature.

In the LT7 unit (Fig. 8a), dominated with sandstone, shale and limestone, the high uranium concentration appears like a spot at numerous points across the unit. The moderate dominance was found in the Central part while the low concentration was experienced in the NW – NE – SS section of the unit. The maximum concentration in the unit is 14 ppm. The tectonic illustration (Fig. 8b) revealed NE part of the unit to be highly peaked and elevated probably due to the shale contribution. IAEA (2003), UNSCEAR (2000) Olowofela et al (2019) opined that uranium concentration tend to be elevated in the sedimentary terrain, if shale is present in the lithological unit. The low uranium concentration region tend to have steep topographical formation. LT8 (Fig. 9a), a weathered basement terrain depicts distribution pattern of uranium concentration such that the low to moderate prevalence are found in the Northern part trending Eastward and Central part of the unit. The high uranium concentration was found in the southerner part of the unit with maximum value of 14 ppm. The Structural distribution of the uranium concentration (Fig. 9b) revealed several anomalous peak across the unit. The chemical weathering have significant effect on the uranium migration since it is mobile in nature.

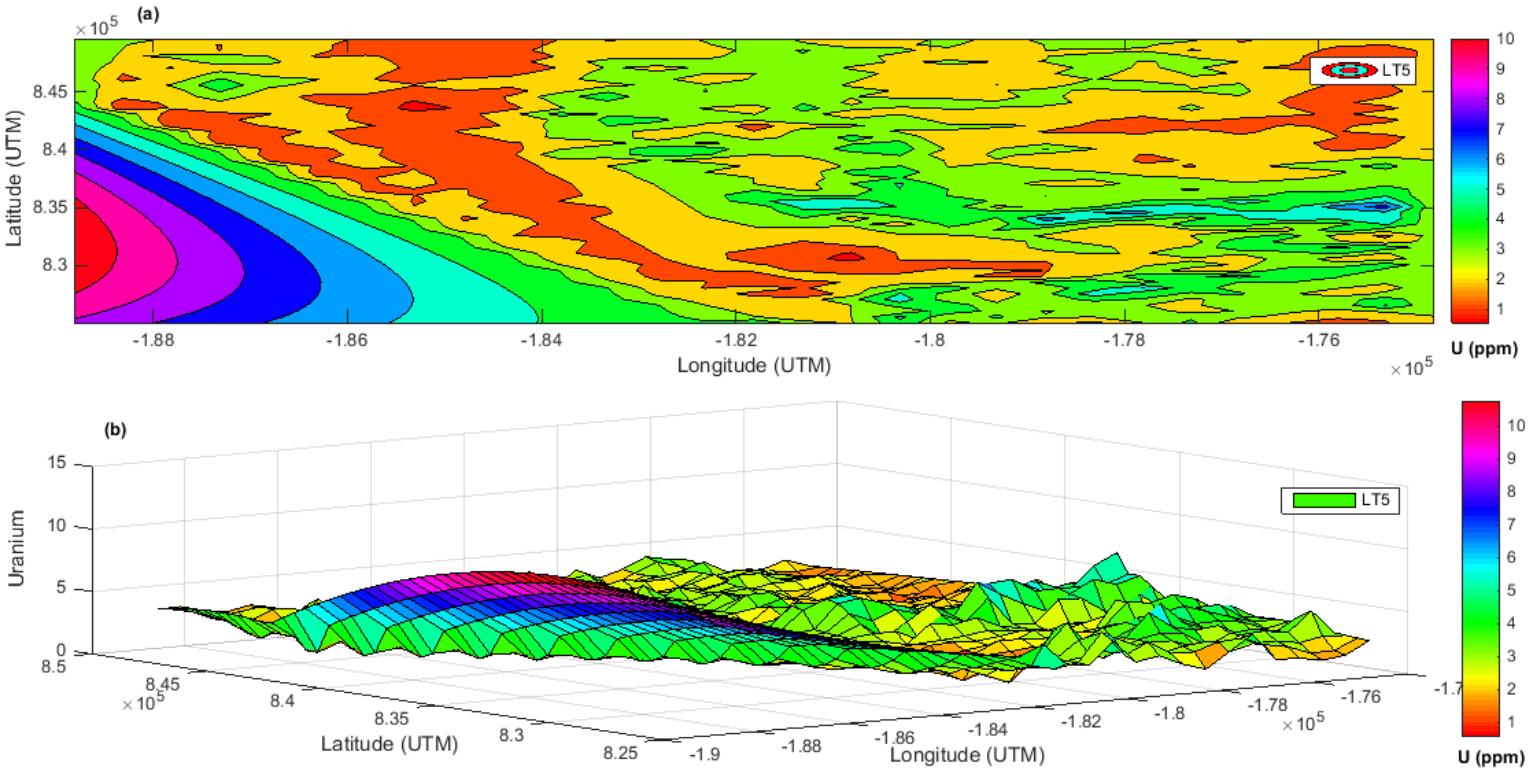

Figure 6: Spatial Surficial representation of uranium distribution in (a) 2D contour (b) 3D surface form of LT5 unit

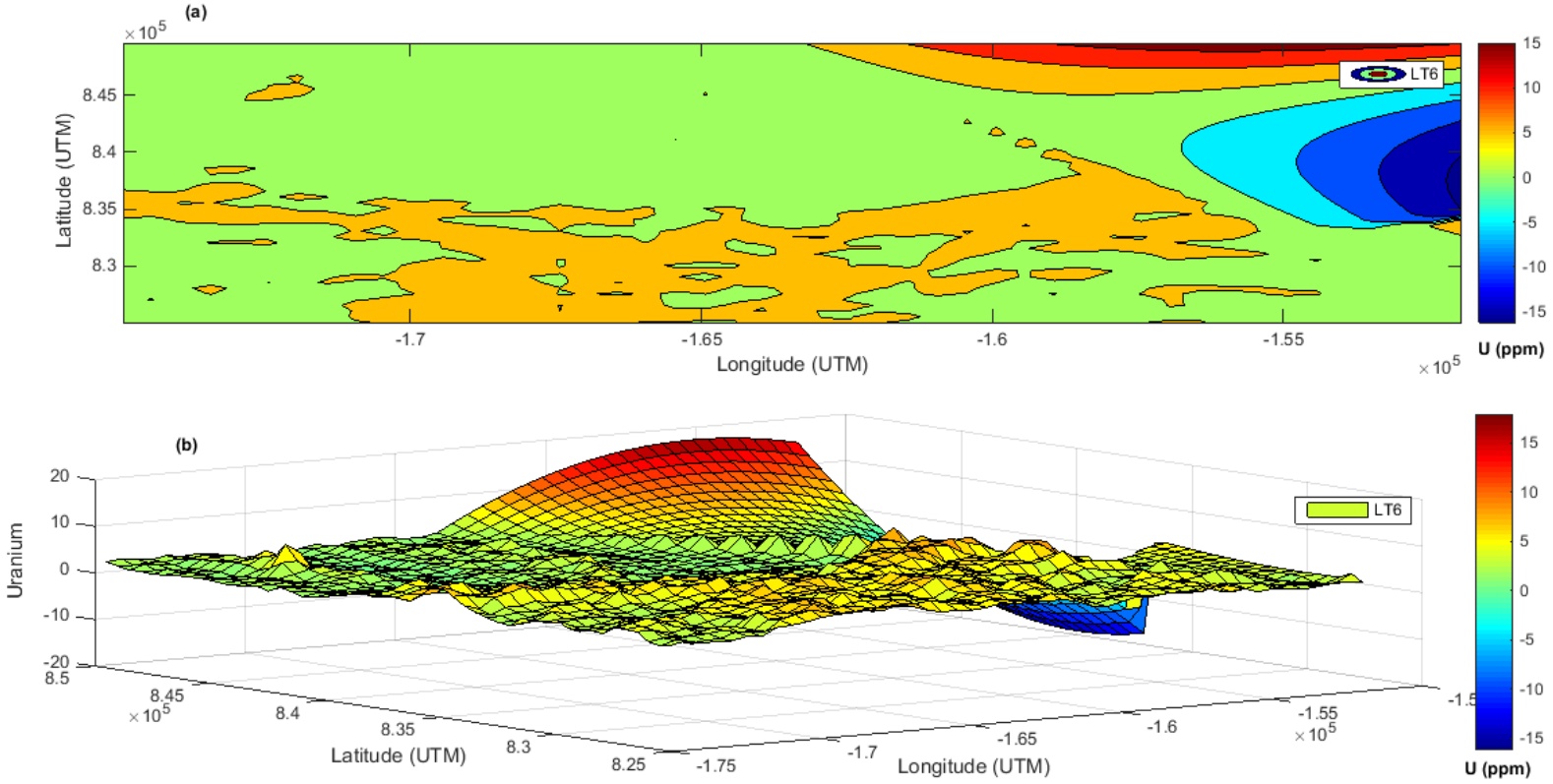

Figure 7: Spatial Surficial representation of uranium distribution in (a) 2D contour (b) 3D surface form of LT6 unit

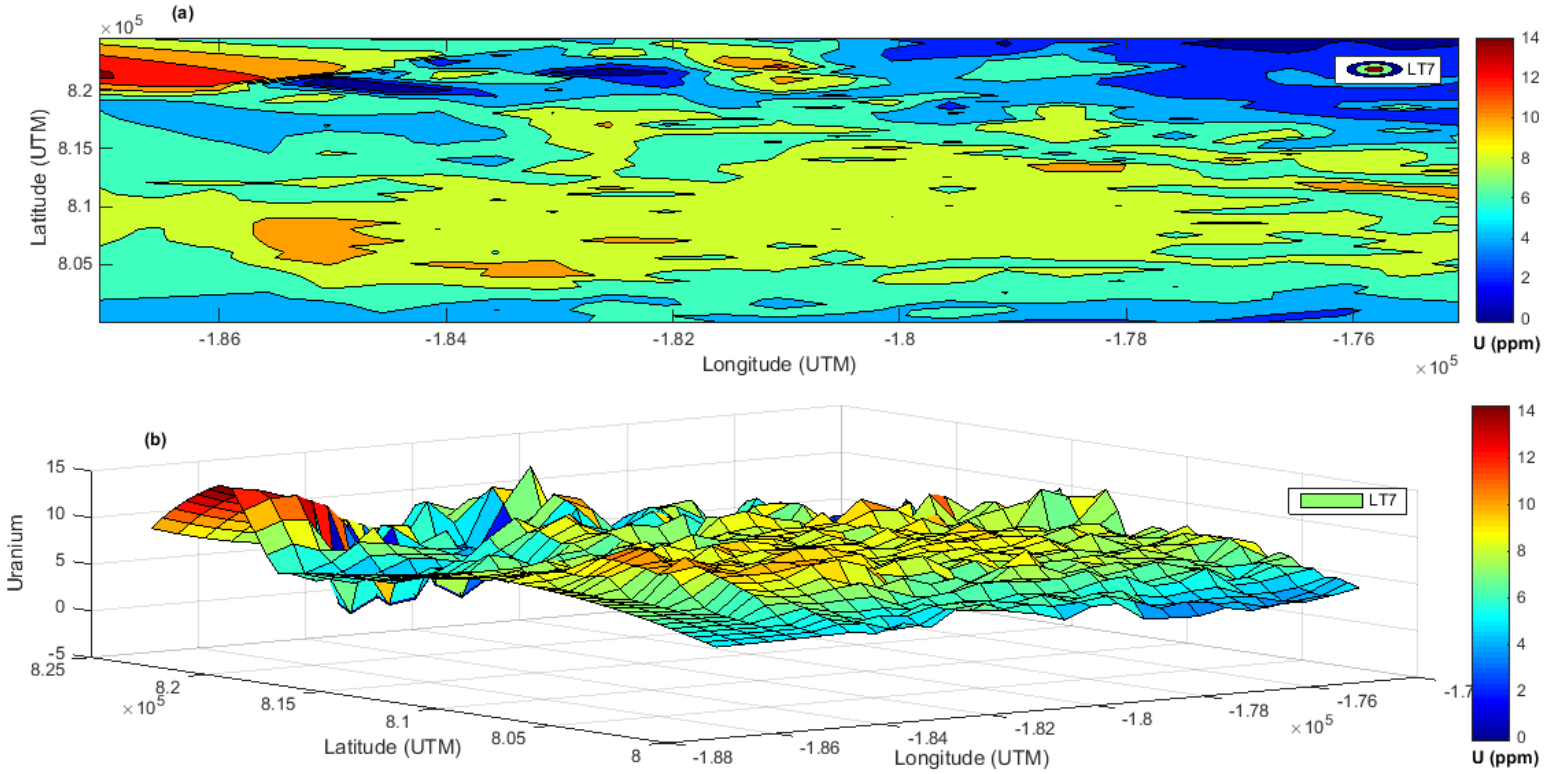

Figure 8: Spatial Surficial representation of uranium distribution in (a) 2D contour (b) 3D surface form of LT7 unit

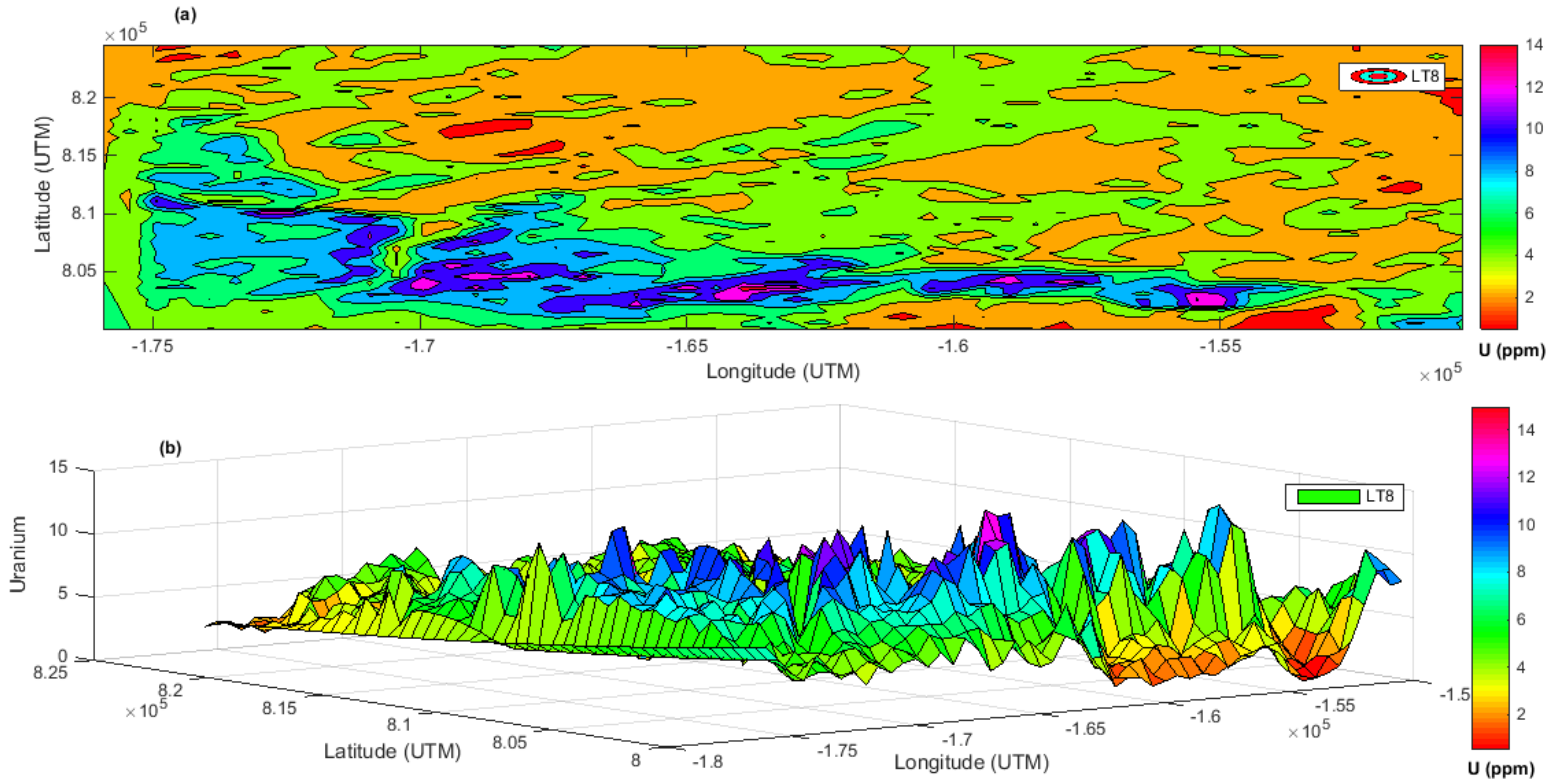

Figure 9: Spatial Surficial representation of uranium distribution in (a) 2D contour (b) 3D surface form of LT8 unit

In the LT9 unit (Fig. 10a) the low concentration of uranium was found to trend in the N – W – SS while the moderate concentration was found in the Central trending East and partly SW corner of the unit. The high uranium prevalence was found like spot in the Eastern part. The surface plot (Fig. 10b) that the region of low concentration was steep with sharp peak while that of high uranium spot have higher elevated sharp peak. The relative maximum uranium distribution in the unit is 12 ppm. The uranium in this unit may be relatively low but the structural feature revealed high level of chemical weathering across the unit. The spatial distribution contour map of uranium in LT10 unit (Fig. 11a) was found to have moderate concentration prevalence across the unit while the low concentration was found in the NW corner and SW – SS section. Figure 11(b) revealed the tectonic feature of the uranium to be steep at NE corner and relatively elevated around upper Northern spot. The topographical uranium response is expected being sedimentary terrain, the uranium tends to percolate (especially if sandstone one of the bedrock composition) due to high porosity.

In the LT11 (Fig. 12a), low uranium concentration was found to also dominate the lithological unit from Central trending N – E – SE. The high prevalence feature was found in the NE corner while the moderate concentration was found in the upper Northern, lower southern and Western part of the unit. The maximum concentration of the unit is 12 ppm. Structurally, a very elevated sharp spot was found in the NE part (Fig. 12b) and partly elevated around N – NW – W of the unit. The low prevalence appears to be uniformly distributed. The spatial distribution of LT12 (Fig. 13a) revealed low concentration in the W – SS and some spot at the Central and Northern part of the unit. The elevated uranium concentration was found at numerous spot embedded within the unit. The structural spatial view of the uranium response to the lithology revealed several high peak anomalous spot associated with moderate – intense uranium concentration (Fig. 13b). The region with high anomalous response may be due to the geochemical weathering resulting into tectonic movement and landslide of the lithological unit.

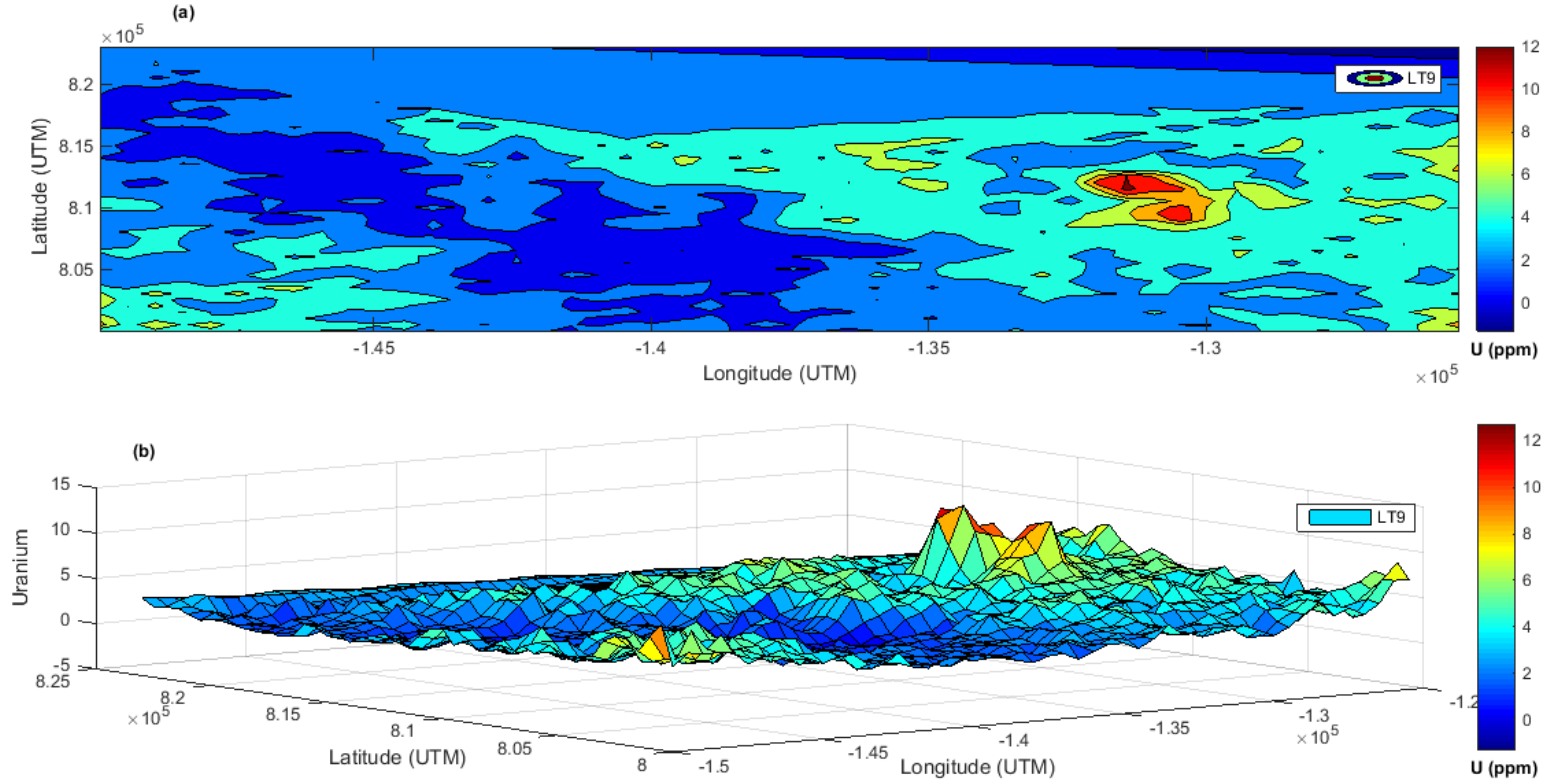

Figure 10: Spatial Surficial representation of uranium distribution in (a) 2D contour (b) 3D surface form of LT9 unit

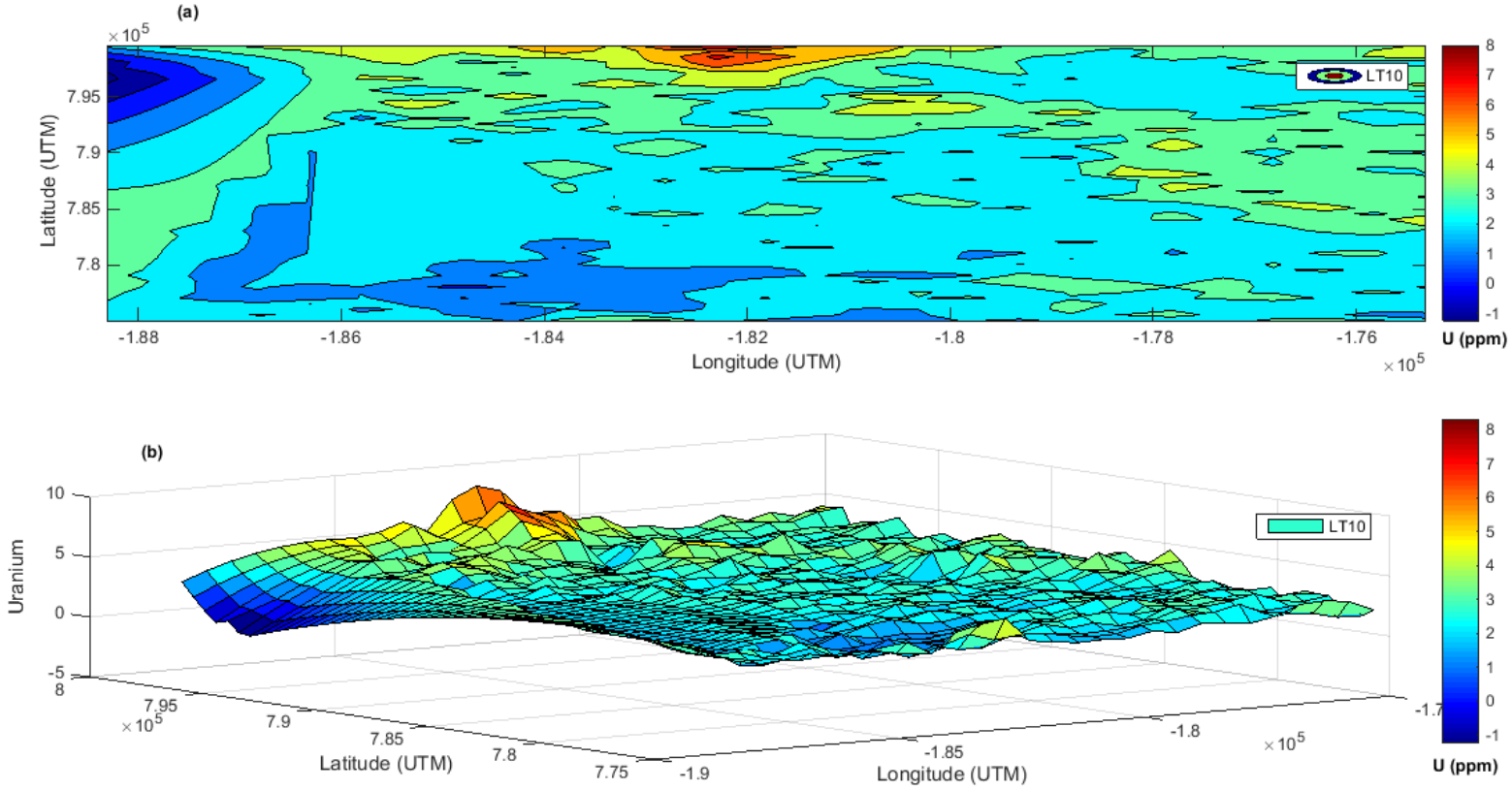

Figure 11: Spatial Surficial representation of uranium distribution in (a) 2D contour (b) 3D surface form of LT10 unit

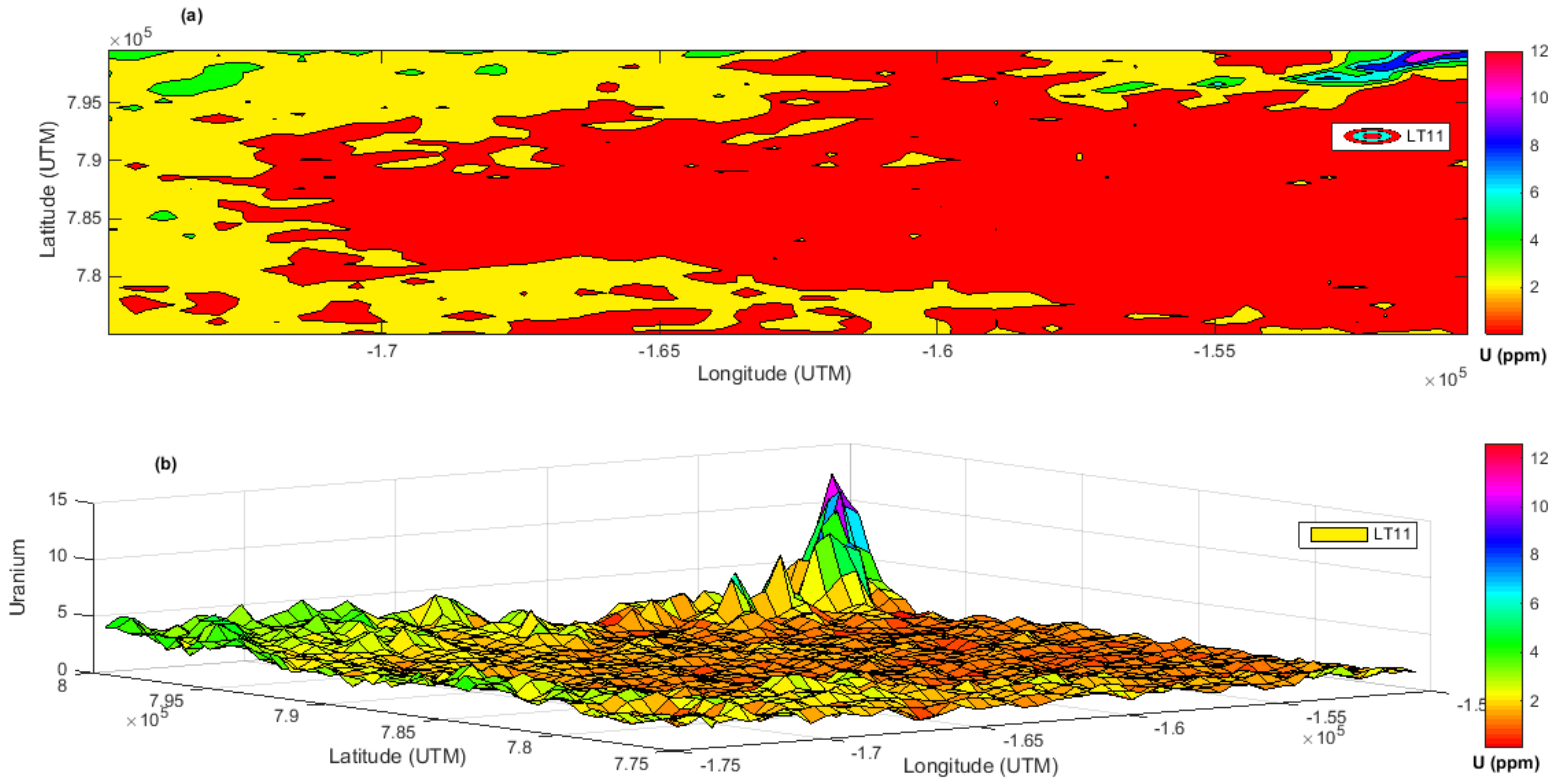

Figure 12: Spatial Surficial representation of uranium distribution in (a) 2D contour (b) 3D surface form of LT11 unit

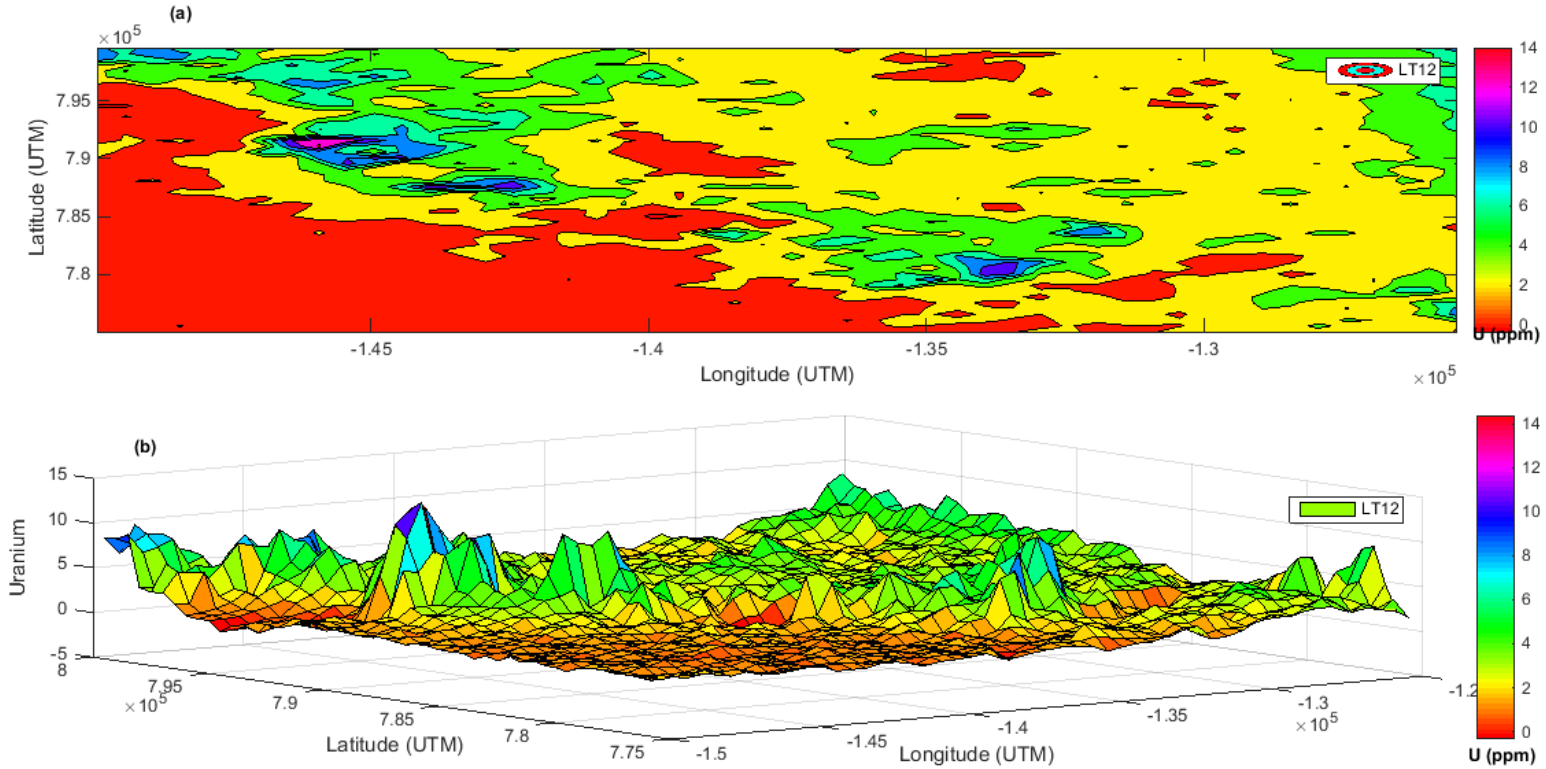

Figure 13: Spatial Surficial representation of uranium distribution in (a) 2D contour (b) 3D surface form of LT12 unit

3.2 Source proximate inferential statistical analysis

The results obtained for the source proximate for the twelve lithological units conducted using inferential statistics was presented in Table 2. The results revealed the source proximate by F – test and T – test to account for common source if the critical value obtained id greater than computed value, otherwise the sources differ.

By F-test analysis, Out of sixty six (66) test conducted, 40 pair of lithological unit to exhibit common sources while 26 differs. LT1 share proximate sources with all other units except LT10 while LT2 differ in source with only three unit (LT3, LT10 and LT11). LT3, LT4, LT8 and LT9 share common source with rest units except two units (LT10 and LT11). LT7 was found to also have common source virtually with all other units except three units (LT8, LT10 and LT11). LT5 revealed disparity of source with unit like LT7, LT8, LT10, LT11 and LT12. In similar contest, LT6 was found to showcase different source with 6 units (LT7, LT8, LT9, LT10, LT11 and LT12). Although LT10 and LT11 were found have source extremely different with other lithological unit, but they still share proximate source with one or two units. LT10 share common source with LT11 and LT12 while LT11 share contiguous source with LT1 and LT12. LT12 was found to have proximate source with all the units except two units (LT5 and LT6).

Using T-test, the result showcased all units to have contiguous source with one another except LT6. The LT6 unit revealed result similar to the F test. Six lithological unit (LT7, LT8, LT9, LT10, LT11 and LT12) were found to have their source different from LT6 unit source. Base on the T-test analysis, Sixty (60) lithological units were found to have proximate source.

From the hypothetical inferences obtained from the F-test and T-test, it can be concluded that F-test suggest multiple or heterogeneous source for the uranium concentrations across all the units while T-test opined similar source virtually across all the twelve lithological units except at LT6 which have distinct source. Most uranium source are attributed to their host bedrock composition which serve as the major force upon which the concentration can be quantify and estimated. Nevertheless, uranium sources may as well be related to the anthropogenic activities and other environmental factors.

Table 2: Summary of F-test and T-test uranium sources proximate statistical analysis

F-test		T-test	
Lithological units	**Hypothesis Remark**	**Lithological units**	**Hypothesis Remark**
LT1	Share common source with all units except LT10	LT1	Share common sources with all units
LT2	Sources differ in LT3, LT10 and LT11 units	LT2	Share common sources with all units
LT3	Share common source with all units except LT10 and LT11	LT3	Share common source with all units
LT4	Share common source with all units except LT10 and LT11 units	LT4	Share common source with all units
LT5	Sources differ in LT7, LT8, LT10 , LT11 and LT12 units	LT5	Share common source with all units
LT6	Sources differ in LT7, LT8, LT9, LT10 , LT11 and LT12 units	LT6	Sources differ in LT7, LT8, LT9, LT10 , LT11 and LT12 units
LT7	Sources differ in LT8, LT10 and LT11 units	LT7	Share common source with all units
LT8	Share common source with all units except LT10 and LT11	LT8	Share common source with all units
LT9	Share common source with all units except LT10 and LT11	LT9	Share common source with all units
LT10	Share common sources only with LT11 and L12	LT10	Share common source with all units
LT11	Share common sources only with LT1 and L12	LT11	Share common source with all units
LT12	Share common source with all units except LT5 and LT6 units	LT12	Share common source with all units

3.3 Factor Analysis

The application of Principal Component Analysis (PCA) to the lithological dataset provides a systematic way of reducing multidimensional variability into fewer, interpretable components, thereby highlighting the dominant geological factors influencing uranium distribution. A total of five principal components (PCs) were extracted, accounting for **68.91% of the cumulative variance (Table 3)**, which is sufficiently robust to describe the underlying geochemical and lithological variability of the study area.

PC1 represents the most significant component, with LT2, LT4, LT7, and LT12 showing strong positive loadings, while LT6 exhibits a weak negative loading with Eigen value 2.586 and percentage variance of 21.553% (Table 3). The positively loaded lithological units are interpreted as the most influential sources or hosts of uranium mineralization. Their strong correlation indicates that uranium is preferentially associated with these lithologies, likely due to favorable mineralogical compositions (felsic intrusives, granitic rocks, or phosphatic horizons) that enhance uranium affinity. The weak negative loading of LT6 suggests either a contrasting lithology (mafic-rich or low-U rocks) or a dilution effect in uranium concentration.

PC2 highlights LT9 and LT11 as strongly positive loading factors and LT6 as negative. PC2 accounted for the Eigen value of 1.904 and percentage variance of 15.863 %.The persistence of LT6 as a negative factor across both PC1 and PC2 strengthens its interpretation as a lithology unfavorable for uranium enrichment. Conversely, LT9 and LT11 appear to play a secondary but significant role in controlling uranium distribution, possibly representing transitional units (contact zones or altered rocks) where uranium has been mobilized and re-deposited along structural conduits.

In PC3, LT8 and LT10 exhibit strong positive loadings with Eigen value of 1.348 and percentage variance of 11.233 %. These units likely represent lithologies with localized uranium enrichment, possibly controlled by secondary alteration processes, hydrothermal inputs, or structural trapping mechanisms. The moderate variance explained by PC3 suggests that these units do not dominate the uranium distribution but contribute meaningfully at a local scale.

LT1 and LT5 load positively in PC4, reflecting another set of lithologies associated with uranium variability. These may represent less dominant but still relevant host rocks, potentially linked to basement granitic intrusions or sediments with minor radioactive contributions. The Eigen value and percentage variance of PC4 are 1.280 and 10.663 %. Their loadings indicate that they act as supporting uranium sources, reinforcing the broader uranium enrichment pattern.

PC5 is characterized by LT3 (positive loading) and LT10 (negative loading) with Eigen value of 1.152 and percentage variance of 9.568 % (Table 3). The strong positive contribution of LT3 suggests it is a specialized lithology with localized uranium potential, while the negative loading of LT10 (also positively loaded in PC3) highlights the complex and possibly heterogeneous role of this unit. This dual behavior may be explained by variations in alteration intensity, mineralogical composition, or depth-related uranium remobilization.

The PCA results reveal that uranium mineralization in the study area is not controlled by a single lithological unit but rather by a suite

of lithologies with varying levels of contribution. The PCA therefore strengthens the interpretation that uranium sources are multi-lithological and structurally influenced, with PC1 capturing the dominant host rocks and subsequent PCs refining the secondary and localized contributors. These insights are critical for exploration targeting, as they guide the prioritization of lithologies and structural settings most favorable for uranium occurrence.

Table 3: Principal component rotated matrix loading factor

Rotated Component Matrix					
Lithological units	Component PC1	PC2	PC3	PC4	PC5
LTU1	-0.283	-0.044	-0.014	**0.783**	0.090
LTU2	**0.722**	-0.020	-0.042	0.003	-0.132
LTU3	-0.009	0.078	0.101	0.006	**0.847**
LTU4	**0.754**	-0.194	-0.041	-0.137	0.391
LTU5	0.259	0.122	0.109	**0.780**	-0.067
LTU6	**-0.470**	**-0.649**	0.204	-0.103	-0.033
LTU7	**0.639**	0.102	0.148	0.011	0.008
LTU8	0.073	0.142	**0.769**	0.199	0.302
LTU9	0.005	**0.843**	0.267	0.069	0.011
LTU10	-0.021	-0.018	**0.681**	-0.081	**-0.535**
LTU11	-0.102	**0.854**	-0.037	-0.032	0.068
LTU12	**0.542**	0.377	-0.424	0.110	-0.071
Eigen value	2.586	1.904	1.348	1.280	1.152
% of Variance	21.553	15.863	11.233	10.663	9.598
Cumulative %	21.553	37.416	48.649	59.312	68.911

3.4 Hierarchical Cluster Analysis

In the Hierarchical Cluster Analysis (HCA), Dendrogram (Figure 14) was adopted to show the hierarchical relationships between the lithological units (LT1–LT12), the result obtained was thereby linked to PCA in such a way as to identify their contributions to airborne uranium concentration through factor loadings. Comparing the two allows us to validate and better interpret the uranium sources.

Three distinct clusters were identified in conjunction with the PCA analysis. Cluster I reflect the Dendrogram groups LT2, LT4, LT7, LT1, LT10 and LT12 into close clusters (Figure 14). These same units were heavily positively loaded in PC1, PC3 and PC4.This confirms that these lithological units are strong uranium-

bearing sources, controlling the dominant variance in uranium distribution.

Cluster II was hierarchical found to have LT9, LT11, LT8, LT5 and LT3 as its constituents. The pair LT9 and LT11 form a tight cluster in the Dendrogram which is linked to PC2 with noticeable properties (positively loaded, Eigenvalue = 1.904; variance = 15.86%) while rest are linked to PC3, PC4 and PC5. These clusters indicate secondary uranium contributors, less dominant than PC1 but still significant

Cluster III shows LT6 as an outlier and negative loaded PCA unit. It appears isolated in the Dendrogram, merging with other units only at a large rescaled distance. This agrees with PCA, where LT6 was consistently negatively loaded in PC1 and PC2. This suggests LT6 is geochemically distinct and not a major uranium source, possibly representing resistant or non-uraniferous lithology.

The integration of PCA and the Dendrogram suggests uranium anomalies are not randomly spread, but clustered along certain lithological domains. The Dendrogram reinforces PCA findings by showing how lithological units with similar uranium contributions group together. The two methods converge on the conclusion that uranium concentration is primarily controlled by a few key lithologies (LT2, LT4, LT7, LT12), with others acting as secondary or negligible contributors.

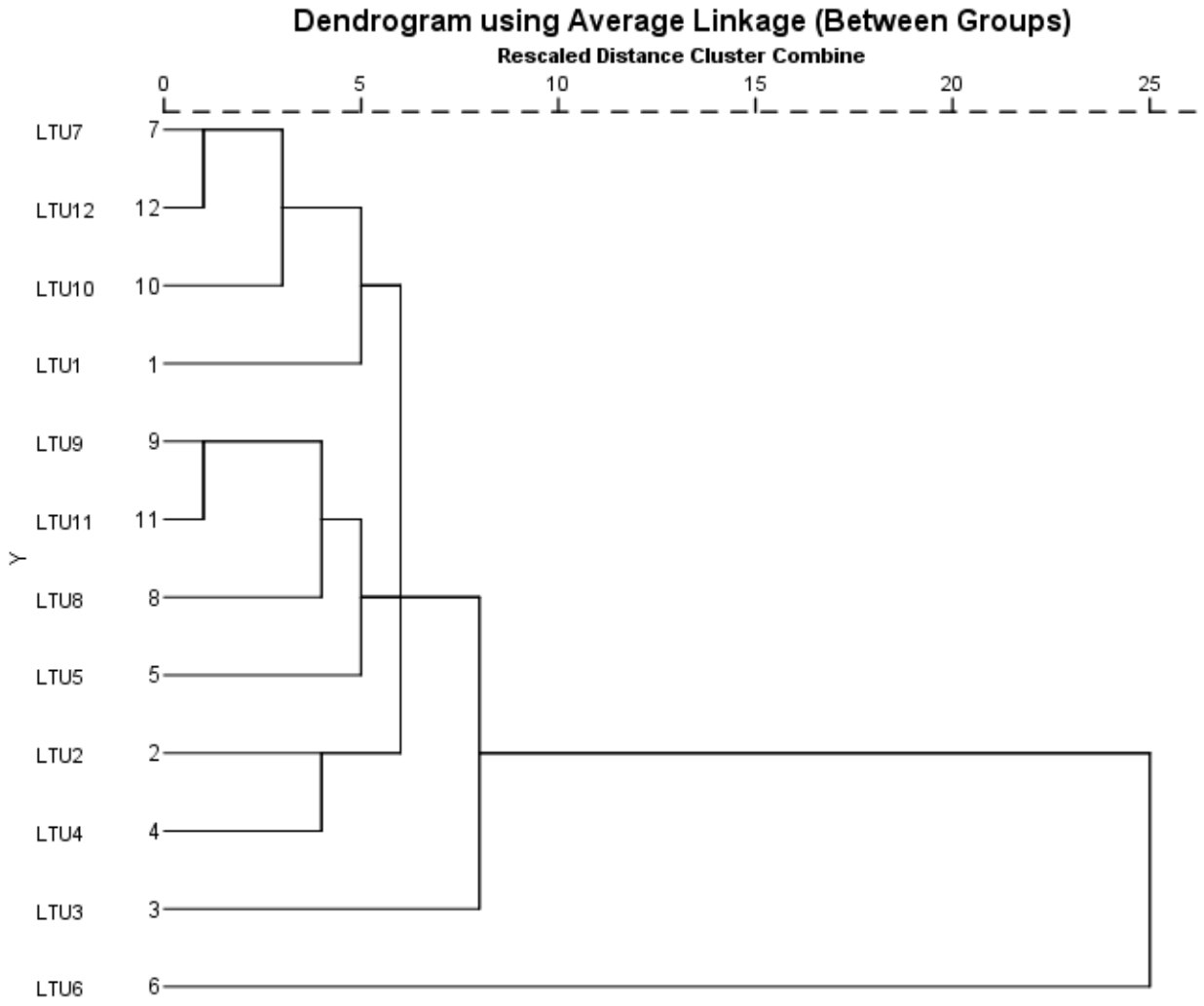

Figure 14: Hierarchical Cluster of uranium units represented with Dendrogram

3.5 Histogram distribution

The histograms give a **frequency distribution of uranium concentration (Figure 15) across the 12 lithological units (LT1–LT12).** LT7, LT8, LT12, and LT9 show multimodal distributions and skewed toward higher uranium concentrations (5–15 ppm) with relatively broad spreads. These units correspond well with the primary uranium source group identified in PCA (PC1 loadings) and the Dendrogram cluster (LT2, LT4, LT7 and LT12). LT7 and LT8, in particular, show long tails extending beyond 10 ppm, suggesting localized uranium enrichment or structural traps. Their multimodal peaks (especially LT9 and LT12) imply heterogeneous uranium distribution, possibly reflecting mixed lithological controls or secondary remobilization.

LT1, LT3, LT4, LT5, LT10, and LT11 display **intermediate uranium concentrations (2–6 ppm)** with unimodal to slightly skewed distributions. These match the **secondary uranium-bearing lithologies** from PCA (PC2 and PC3) and form the secondary clusters in the Dendrogram. LT1 and LT3 show fairly symmetrical bell-shaped curves, suggesting

uniform background uranium content typical of moderately enriched lithologies. LT11 and LT10 have sharp peaks near **2–3 ppm**, indicating **restricted uranium occurrence** likely controlled by specific geochemical environments.

LT2 and LT6 show relatively **narrower ranges and lower peak concentrations** (minimal sources). LT2, although clustered with uranium-rich lithologies in the Dendrogram, displays a tight concentration range (3–5 ppm), suggesting it contributes **less significantly** than LT7 and LT12. LT6 is distinctive, with a broad flat-topped distribution between 2–8 ppm, reflecting **geochemical uniformity but low uranium enrichment.** This agrees with PCA, where LT6 was negatively loaded, confirming its **minor uranium source role**

The histograms reveal that uranium concentration is unevenly distributed across lithological units. The **primary uranium hosts (LT7, LT8, LT9, LT12)** show higher and broader concentration ranges, while others contribute background levels. These patterns are consistent with PCA and Dendrogram results, reinforcing the interpretation that uranium anomalies are structurally and lithologically controlled in Western Ogun State.

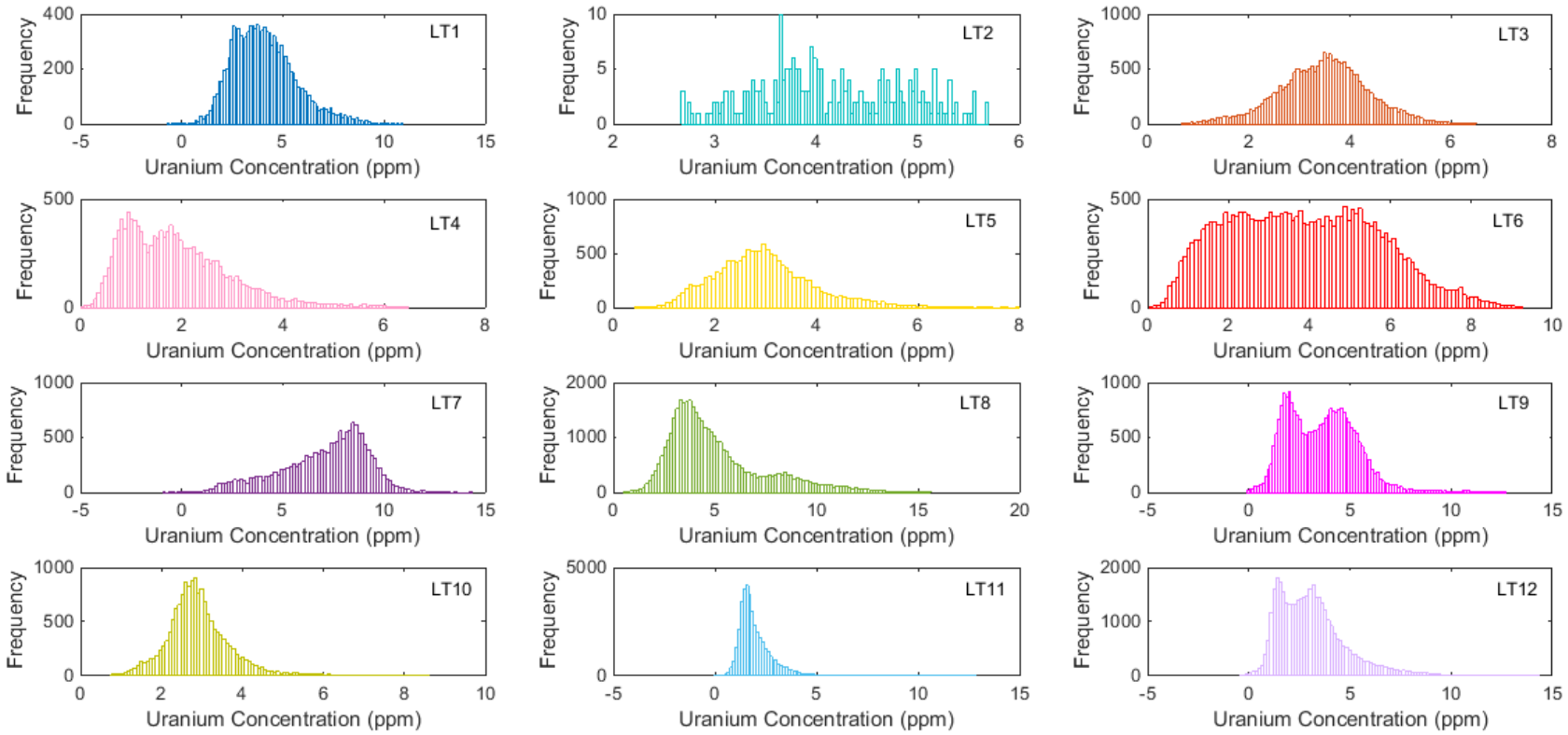

15: Histogram distribution of uranium concentration validating the source proximate

4.0 Conclusion

In this study, the spatial distribution and source proximate analysis were investigated for the uranium concentration in the Western part of Ogun State and the following deductions were made:

(i) The spatial construction revealed the abundance of uranium concentration in the region with anomalous response to the lithological units.
(ii) The Inferential analysis for F-test gives detailed information compared to T-test
(iii) LT6 gives similar hypothetical report for both F -test and T- test.
(iv) The Principal component analysis revealed positive loaded factor for all the lithological unit component except LT6.
(v) The Hierarchical cluster analysis result was found in consonance with that Inferential test and principal component analysis
(vi) The histogram accounted for multimodal distribution in the major uranium controlling source units while LT6 has a minimal source.

Conclusively, the spatial and source proximate analysis carried out have shown that virtually all the lithological unit have uranium concentration in moderate quantity which may be considered for economic benefit and exploration.

Acknowledgements

The Author wish to appreciate the Nigeria Geological Survey Agency for the airborne uranium data. Special appreciation goes to the Cartographer who help in providing detailed Geological map of the study area.

Declaration of competing interest

The authors declare that they have no known competing financial interests or personal relationships that could have appeared to influence the work reported in this paper.

References

Abdulsalam, N. N., John, F. O., & Ologe, O. (2023). Effects of magnetic and radiometric responses on hydrothermal zones in part of Nasarawa, North-Central Nigeria. *Journal of Tropical Resources and Sustainable Science, 11*(1), 29–36.

Adegoke, O. S., & Omatsola, E. (2015). Airborne radiometric survey for uranium exploration in the Sokoto Basin, Nigeria. *Journal of African Earth Sciences, 101*, 257–265.

Adewoyin, O. O., Omeje, M., Onumejor, C. A., Adagunodo, T. A., Ndubuisi, A. O., Nwaluka, V. O., Akinpelu, A., & Joel, E. S. (2019). Mapping of Uranium-238 deposit and its contribution to indoor radon gas in Ota, Ogun State, Nigeria. *International Conference on Energy and Sustainable Environment*.

Ammar, A. A., Abdelhady, H. M., Soliman, S. A., & Sadek, H. S. (1988). Aerial radioactivity of phosphate in the western central eastern Desert of Egypt. *Earth Science, 1*, 181–203.

Badmus, B. S., Olatinsu, O. B., & Idowu, O. A. (2010). Hydrogeophysical

evaluation of the groundwater potential of Ajegunle–Ilo, Southwestern Nigeria. *Journal of Geology and Mining Research, 2*(7), 155–163.

Ezekiel, K., & Nur, A. (2023). Analysis of high-resolution aeroradiometric data over Sokoto Basin and adjoining areas, northwestern Nigeria. *IRESPUB Journal of Natural & Applied Sciences, 2*(2), 84–92.

Faruwa, A. R., Olatunji, S. O., Adepelumi, A. A., & Akinlabi, O. (2021). Airborne magnetic and radiometric mapping for litho-structural control of bitumen deposit, southwestern Nigeria. *Journal of African Earth Sciences, 181*, 104238. https://www.sciencedirect.com/science/article/abs/pii/S1464343X21001230

IAEA. (2003). *Guidelines for radioelement mapping using gamma ray spectrometry data*. International Atomic Energy Agency, Vienna. IAEA-TECDOC-1363.

Idi, B. Y., Ofulume, A. B., & Kwaya, M. Y. (2020). Mapping ground exposure rate and external hazard index from pre-processed aeroradiometric data (Sheet 145), Nigeria basement complex. *European Journal of Environment and Earth Sciences, 1*(3), 17–24. https://www.ej-geo.org/index.php/ejgeo/article/view/59

Jegede, D. O., Afolabi, T. A., Agunbiade, F. O., et al. (2025). Spatial distribution and radiological hazards assessment of naturally occurring radionuclide materials in soil from quarry sites in Ogun State, Nigeria. *Environmental Monitoring and Assessment, 197*, Article 575. https://doi.org/10.1007/s10661-025-13988-

Kogbe, C. A. (1989). *Geology of Nigeria* (2nd ed.). Rock View International.

Nigerian Geological Survey Agency (NGSA). (2019 *Geological map of Nigeria*. NGSA.

Ngwaka, I. F., Ogbukagu, I. C., & Okeke, O. C. (2023). Interpretation of aeroradiometric data of part of Lower Benue Trough, Nigeria. *European Journal of Environment and Earth Sciences, 4*(3), 9–18. http://dx.doi.org/10.24018/ejgeo.2023.4.3.394

Ogungbemi, O. S., Adelusi, A. O., Akinlabi, O., Olasunkanmi, N. K., & Afolabi, O. (2021). Airborne and ground geophysical evaluation of potential mineralization targets in parts of the Ilesha Schist Belt, SW Nigeria. *Interpretation, 9*(3), T663–T677. https://library.seg.org/doi/10.1190/int-2021-0012.1

Ogunsanwo, F. O., Olowofela, J. A., Okeyode, I. C., Idowu, O. A., & Olurin, O. T. (2019). Aeroradiospectrometry in the spatial

formation characterization of Ogun State, South-Western Nigeria. *Scientific African, 6*, e00204. https://doi.org/10.1016/j.sciaf.2019.e00204

Ogunsanwo, F. O., Ozebo, V. C., Olurin, O. T., Ayanda, J. D., Coker, J. O., Sowole, O., Ogunsanwo, B. T., Olumoyegun, J. M., & Olowofela, J. A. (2021). Geostatistical analysis of uranium concentrations in north-western part of Ogun State, Nigeria. *Journal of Environmental Radioactivity, 237*, Article 106681. https://doi.org/10.1016/j.jenvrad.2021.106681

Ogunsanwo, F. O., Ayanda, J. D., Mustapha, A. O., Olatunji, A. S., Ozebo, V. C., Olurin, O. T., Alaka, A. O., Okeyode, I. C., Adepitan, J. O., & Olowofela, J. A. (2023). Empirical relation between magnetic and radiometric survey in bitumen area, Ogun State, Nigeria. *Materials and Geoenvironment*. https://doi.org/10.2478/rmzmag-2023-0003

Okeyode, I. C., & Olurin, O. T. (2018). Radiometric survey in geological mapping of parts of basement complex area of Nigeria. *Vietnam Journal of Earth Sciences, 40*(3), 244–259.

https://colab.ws/articles/10.15625%2F0866-7187%2F40%2F3%2F12619

Oladunjoye, M. A., &Ademila, O. (2015). Radiometric survey for uranium mineralization in part of Southwestern Nigeria. *Journal of African Earth Sciences, 108*, 42–55.

https://doi.org/10.1016/j.jafrearsci.2015.04.004

Oladunjoye, M. A., Olayinka, A. I., & Odukoya, A. M. (2016). Geophysical mapping of basement structures in relation to uranium mineralization in parts of Southwestern Nigeria. *Journal of Applied Geophysics, 131*, 1–12. https://doi.org/10.1016/j.jappgeo.2016.05.002

Ologe, O., Moyi, A. M., Sanusi, F., Tsafe, U. H., & Umar, S. (2024). Interpretation of airborne radiometric data of a typical basement complex, Northwest Nigeria. *Arid Zone Journal of Engineering, Technology and Environment, 20*(2), 294–307. https://www.azojete.com.ng/index.php/azojete/article/download/1032/601/

Olowofela, J. A., Okeyode, I. C., Idowu, O. A., Olurin, O. T., & Ogunsanwo, F. O. (2019). Lithological mapping of Ogun State, southwestern Nigeria, using aeroradiospectrometry. *Environmental Earth Sciences, 78*(8), Article 233. https://doi.org/10.1007/s12665-019-8256-6

Omatsola, M. E., & Adegoke, O. S. (1981). Tectonic evolution and Cretaceous stratigraphy of the Dahomey Basin. *Journal of Mining and Geology, 18*(1), 130–137.

Onyejiuwaka, I. S., & Nkiru, N. C. (2020). Application of airborne radiometric method in geologic mapping of Malufashi area and environs, Northwestern Nigeria. *International Journal of Advanced Geosciences, 8*(2), 179–185. https://doi.org/10.14419/ijag.v8i2.31071

Paul, S. N., Oko, I. J., Olatunji, M. A., & Adedayo, O. M. (2022). Natural occurring radioactive materials (NORMs) from mining in Nigeria: A systematic review. *Journal of Environmental Radioactivity, 253–254*, 106994. https://www.sciencedirect.com/science/article/abs/pii/S0265931X22000790

Rahaman, M. A. (1976). Review of the basement geology of Southwestern Nigeria. In C. A. Kogbe (Ed.), *Geology of Nigeria* (pp. 41–58). Elizabethan Publishing Co.

Telford, W. M., Geldart, L. P., & Sheriff, R. E. (1990). *Applied geophysics* (2nd ed.). Cambridge University Press. https://doi.org/10.1017/CBO9781139167932

UNSCEAR. (2000). *Sources and effects of ionizing radiation: United Nations Scientific Committee on the Effects of Atomic Radiation 2000 Report to the General Assembly*. United Nations.

Wara, M., Danbatta, U. A., & Yakubu, I. (2021). Estimation of radioelements concentration in Sokoto Basin using high-resolution aeroradiometric data. *World Journal of Advanced Research and Reviews, 10*(3), 189–198. https://wjarr.com/sites/default/files/WJARR-2021-0514.pdf

Youssef, M. A. S. (2016). Relationships between ground and airborne gamma-ray spectrometric survey data, North Ras Millan, Southern Sinai Peninsula, Egypt. *Journal of Environmental Radioactivity, 152*, 75–84. https://doi.org/10.1016/j.jenvrad.2015.09.008